Environmental Pollution 266 (2020) 115423

Contents lists available at ScienceDirect

Environmental Pollution

journal homepage: www.elsevier.com/locate/envpol

# Cylindrospermopsin is effectively degraded in water by pulsed corona-like and dielectric barrier discharges☆

Marcel Schneider [a, *], Raphael Rataj [b], Juergen F. Kolb [b], Luděk Bláha [a]

[a] RECETOX, Faculty of Science, Masaryk University, Kamenice 753/5, 62500, Brno, Czech Republic
[b] Leibniz Institute for Plasma Science and Technology e.V. (INP Greifswald), Felix-Hausdorff-Straße 2, 17489, Greifswald, Germany

ARTICLE INFO

*Article history:*
Received 24 February 2020
Received in revised form
22 June 2020
Accepted 11 August 2020
Available online 15 August 2020

*Keywords:*
Cyanotoxin
CYN
DBD
Drinking water treatment
Non-thermal plasma

ABSTRACT

Cylindrospermopsin (CYN) is an important cyanobacterial toxin posing a major threat to surface waters during cyanobacterial blooms. Hence, methods for cyanotoxin removal are required to confront seasonal or local incidences to sustain the safety of potable water reservoirs. Non-thermal plasmas provide the possibility for an environmentally benign treatment which can be adapted to specific concentrations and environmental conditions without the need of additional chemicals. We therefore investigated the potential of two different non-thermal plasma approaches for CYN degradation, operated either in a water mist, i.e. in air, or submerged in water. A degradation efficacy of 0.03 ± 0.00 g $kWh^{-1}$ $L^{-1}$ was found for a dielectric barrier discharge (DBD) operated in air, while a submerged pulsed corona-like discharge resulted in an efficacy of 0.24 ± 0.02 g $kWh^{-1}$ $L^{-1}$. CYN degradation followed a pseudo zeroth order or pseudo first order reaction kinetic, respectively. Treatment efficacy of the corona-like discharge submerged in water increased with pH values of the initial solution changing from 5.0 to 7.5. Notably, a pH-depending residual oxidative effect was observed for the submerged discharge, resulting in ongoing CYN degradation, even without further plasma treatment. In this case hydroxyl radicals were identified as the dominant oxidants of CYN at acidic pH values. In comparison, degradation by the DBD could be related primarily to the generation of ozone.



## 1. Introduction

Cyanobacteria are bloom-forming phototrophic prokaryotes capable of producing a wide range of toxic secondary metabolites, known as cyanotoxins. Due to the increased eutrophication of surface waters, toxic cyanobacterial blooms occurred more frequently in recent years, including e.g. massive harmful algal blooms and toxicity outbreaks in USA and worldwide (Brooks et al., 2016). This consequently increases the risk for cyanotoxins, such as the hepatotoxic cylindrospermopsin (CYN), to contaminate drinking water (Blahova et al., 2009; Vanova et al., 2019). In 1979, more than 100 people were hospitalized in Queensland, Australia after showing various symptoms of gastroenteritis. The incident was linked to the water supply which periodically experienced cyanobacterial blooms dominated by non-toxic *Anabaena circinalis* and toxic *Cylindrospermopsis raciborskii*, from which the alkaloid CYN was isolated (Griffiths and Saker, 2003). So far, the World Health Organization has not proposed guideline values for CYN but is aware of its potential risk. Thus, the upcoming update of their Guidelines for Drinking-water Quality is expected to include recommendations for CYN (updates can be found on the homepage (WHO, 2020)). Since CYN can be reasonably stable in surface water, a half-life of up to several weeks has been reported (Ministry of Health, 2017), more rigorous treatment approaches are required to remove the hepatotoxin.

The occurrence of cyanobacteria and related toxins in drinking water can be prevented or mitigated by various measures including water abstraction management, biomanipulation, nutrient control, artificial destratification and the application of algaecides (Ibelings et al., 2016). However, the risk of unintentional release of intracellular cyanotoxins from cyanobacterial cells, or other economic and technical disadvantages limit the success of these strategies. In addition, water scarcity and climate change further encourage the investigation of more advanced treatment technologies.

☆ This paper has been recommended for acceptance by Sarah Harmon.

* Corresponding author.
*E-mail addresses:* marcel.schneider@recetox.muni.cz, marcel.schneider90@outlook.com (M. Schneider), raphael.rataj@inp-greifswald.de (R. Rataj), juergen.kolb@inp-greifswald.de (J.F. Kolb), ludek.blaha@recetox.muni.cz (L. Bláha).

https://doi.org/10.1016/j.envpol.2020.115423

Cyanotoxin removal at full-scale drinking water treatment facilities often includes traditional approaches, such as activated carbon filtration, biodegradation, chlorination or ozonation, with varying degrees of success (Westrick and Szlag, 2018). For CYN removal from drinking water, various treatment methods have already been studied. For example, biodegradation (Ho et al., 2012), passive physical removal by nanofiltration (Dixon et al., 2011), activated carbon (Ho et al., 2008) or sediments (Klitzke et al., 2011), chemical oxidation and advanced oxidation processes (AOPs) were investigated to remove CYN. Traditionally employed oxidants like chlorine and ozone effectively degrade CYN depending on pH, initial oxidant concentration and the reaction time. Conversely, chlorine dioxide, monochloramine and permanganate were shown to be ineffective against CYN (Ho et al., 2008; Onstad et al., 2007; Rodríguez et al., 2007). However, in the presence of natural organic matter or bromide, chlorine and ozone can produce toxic disinfection byproducts such as trihalomethans and bromates (Rodríguez et al., 2007). AOPs on the other hand promote the *in situ* formation of highly reactive radicals, e.g. •OH and other reactive chemical species. AOPs such as photocatalysis (Zhang et al., 2015), UV in combination with $H_2O_2$, $S_2O_8^{2-}$ or $HSO_5^-$ (He et al., 2014a, 2014b), $TiO_2$-catalyzed ozonation (Wu et al., 2015), Fenton reaction (Liu et al., 2018) and electrochemical oxidation (Bakheet et al., 2018) have been studied.

Amongst AOPs, non-thermal plasmas (NTPs) recently received a lot of attention for their potential application in water (Banaschik et al., 2015; Magureanu et al., 2018) and air purification (Schiavon et al., 2017; Xia et al., 2019). NTPs are generated by electric discharges in water or in gas under atmospheric or low pressure without the need of any other consumables. Even recalcitrant compounds, which appeared to be either persistent or only somewhat susceptible to conventional and other advanced treatment approaches, could effectively be degraded (Banaschik et al., 2015). Depending on the design of a plasma source, a range of reactive species can be formed *in situ*, e.g. •OH, $H_2O_2$, $O_3$, NO•, as well as electrons, photons, excited molecules, atoms and ions. The type and quantity of the generated species is determined by the discharge configuration and the operating medium (Scholtz et al., 2015). Accordingly, plasma treatments can be selected and optimized with respect to the most promising degradation mechanism of a specific compound. A further advantage of plasma treatment is that hydroxyl radicals can be generated directly from water without the need of catalysts or precursors such as $TiO_2$ or hydrogen peroxide in combination with UV radiation. In contrast to UV-based AOPs, the generation of reactive species by NTPs does not rely on UV irradiance and is thus not affected by the turbidity of the treated water and the penetration depth of the UV light. Consequently, as no additional reagents or catalysts are required to produce reactive species, NTPs can be considered an environmentally benign technology. Likewise, in comparison to traditional ozonation, where ozone is produced by a dielectric barrier discharge (DBD) in gas which is then injected into water, the immersion of water droplets directly into the plasma volume of a gas-phase DBD permits an instantaneous delivery of ozone and other reactive species to the pollutants contained and distributed in the droplets.

Despite their potential and advantages, research on cyanotoxin degradation by NTPs so far is scarce and limited to microcystin (Zhang et al., 2016), anatoxin-a (Jo et al., 2016) and β-*N*-methylamino-L-alanine (Nisol et al., 2019). Comparison of different plasma sources in this context has not been reported at all and previous studies mainly focused on gas-liquid interfacial or gas-phase plasma systems.

In the present study, we focused particularly on the comparison of a pulsed corona-like discharge submerged in water and a DBD in air with water droplets to assess the CYN degradation efficacies. Both plasma sources were chosen based on previous experience for the degradation of pollutants. For the DBD, the anticipated mechanism of action is based on the immediate and efficient delivery of ozone. Therefore, water is dispersed in droplets in an aerosol to increase the interaction area between plasma and the contaminated water volume. The corona-like discharge submerged in water exploited a different principle and mechanism. In this case, especially short-lived hydroxyl radicals were provided throughout the treated volume by plasma filaments. The aim of this investigation and comparison was to develop, on the one hand, a basic understanding of relevant mechanisms for plasma treatment with respect to different underlying reaction mechanisms and, on the other hand, to provide design criteria for associated future developments of treatment systems. Accordingly, CYN degradation kinetics and mechanisms for both discharges were compared to evaluate CYN removal as well as the formation of potential degradation products and reactive species. Concurrently, the effects of operating voltage, wire diameter and solution pH on the degradation efficacy were evaluated to provide guidance with respect to technological developments. This study provides, to the best of our knowledge, for the first time the necessary results for a comparison of degradation mechanisms under defined conditions for fundamentally different NTPs and with respect to their potential application.

## 2. Materials and methods

### 2.1. Standards and reagents

CYN (≥95%) was obtained from Enzo Life Sciences, Inc. and used to record the calibration curve for CYN quantification as well as for determination of CYN extract purity. $H_2O_2$ (30%, w/w) was purchased from Merck KGaA. Titanium(IV) oxysulfate − sulfuric acid solution (27−31% $H_2SO_4$ solution) and para-chlorobenzoic acid (pCBA, 99%) were obtained from Sigma-Aldrich. Methanol (Rotisolv® HPLC Gradient) and acetonitrile (Rotisolv® Ultra LC-MS grade) were obtained from Carl Roth. Water (LC-MS Ultra-Chromasolv for UHPLC-MS) was obtained from Honeywell Riedel-de Haën and formic acid was obtained from Fluka Analytical.

The method used for CYN extraction from freeze-dried *Aphanizomenon flos-aquae* (PCC 7905) biomass was adapted from Cerasino et al. (2016). In short, approximately 10 g of biomass were separated into 100 mg aliquots and extracted with 75% methanol each (10 mL per 100 mg biomass), sonicated on ice for 30 min and centrifuged at 3400×*g* for 10 min. The procedure was repeated and supernatants from both steps were pooled. The methanolic extract was dried on a rotary evaporator at 55 °C, re-dissolved in Milli-Q water and centrifuged using 0.22 μm cellulose acetate spin filters (National Scientific) at 7400×*g* for 10 min. The extract was subjected to Extract Clean Carbograph SPE columns (500 mg/8 mL, Grace) and eluted with 5:9.5:85.5 formic acid:-dichlormethane:methanol. The eluate was again dried on a rotary evaporator and re-dissolved in Milli-Q water. Subsequently, CYN was further purified by preparative HPLC (Agilent 1100 Series, Agilent Technologies) on a C18 XBridge Prep column (10 × 100 mm, 5 μm, Waters) using a gradient elution with acidified water (0.1% formic acid) and acetonitrile (for details see Supplementary Table S1) as well as a fractionator (Agilent 1200 Series, Agilent Technologies). CYN was detected at 262 nm, fractions were pooled, dried using a $N_2$ stream at 50 °C and re-dissolved in Milli-Q water prior to experiments. Based on the comparison of UV spectra of the purified CYN with the purchased standard, purity of isolated CYN was estimated to approximately 70%.

### 2.2. Chemical analysis

In the first set of experiments, CYN reduction was quantified by an Agilent 1200 Infinity Series HPLC coupled with an Agilent 1260 DAD detector (Agilent Technologies) at $\lambda = 262$ nm. Chromatographic separation was performed on an InfinityLab Poroshell 120 SB-AQ column (2.1 × 100 mm, 2.7 μm, Agilent Technologies) equipped with an InfinityLab Poroshell 120 SB-AQ guard column (2.1 × 5 mm, 2.7 μm, Agilent Technologies) and gradient elution with acidified water (0.1% formic acid) and acetonitrile (for details see Supplementary Table S2). For the study of the degradation kinetics and mechanisms, an Agilent 6130 quadrupole MS detector (Agilent Technologies) was used in addition, connected to the outlet of the DAD detector, to follow the formation of potential CYN degradation products. The MS detector was operated in scan mode (*m/z* 100−500 Da) and positive electrospray ionization. Gradient elution was adjusted for better separation of product peaks (for details see Supplementary Table S3). pCBA was used as •OH probe and quantified by HPLC-DAD on the same column at $\lambda = 238$ nm and isocratic elution with 60% acidified water (0.1% formic acid) and 40% acetonitrile at a flow of 0.6 mL $min^{-1}$. $H_2O_2$ was quantified colorimetrically with titanium(IV) oxysulfate. Upon the reaction of $H_2O_2$ with titanium(IV) oxysulfate under acidic conditions, the initially colorless solution produces a yellow color, for which the intensity was determined at $\lambda = 407$ nm photometrically (Banaschik et al. (2017) and references cited therein).

### 2.3. Plasma reactors

#### 2.3.1. Corona-like discharge in water

Corona-like discharges in water were instigated in a cylindrical electrode geometry in which two intertwined tungsten (99.95% purity, Goodfellow) wires were coaxially surrounded by a grounded stainless steel mesh (0.5 mm mesh size, 200 μm wire diameter) (Supplementary Fig. S1). Streamers were generated along the entire length of the wires upon application of high voltage pulses. Positive high voltage pulses were applied to the wires from a 6-stage Marx bank pulse generator with a pulse duration of 390 ± 50 ns (determined as full width at half maximum at a frequency of 20 Hz; see Supplementary Fig. S2 for an example of an applied pulse). Voltage and current pulses were recorded using a passive high voltage probe (P6015A, Tektronix) and a Rogowski-coil (Model 2878, Pearson) connected to an oscilloscope (WaveSurfer 64MXs-B, LeCroy). The tungsten wires were replaced after every experiment to ensure reproducibility. The total reactor volume of 135 mL was completely filled. The sample solution was cooled to 20 and continuously circulated through the reactor from bottom to top using a peristaltic pump at 50 mL $min^{-1}$ to prevent atmospheric air from entering into the reactor. Air bubbles inside the reactor needed to be avoided to inhibit unwanted electrical breakdowns in the system which would damage the reactor.

#### 2.3.2. DBD in air with water droplets

A DBD was operated in ambient air between two layers of tungsten rod electrodes (purity 99.9%, diameter 2 mm) as shown in Supplementary Fig. S3. The grounded rods in the bottom layer were covered by quartz tubes (diameter 4 mm, wall thickness 0.8 mm). Negative high voltage pulses were applied to the bare rods in the top layer with a pulse duration of 400 ± 60 ns (determined as full width at half maximum at a frequency of 1 kHz (Eagle Harbor High Voltage Pulse Generator NSP-120-20-N); see Supplementary Fig. S4 for an example of an applied pulse). Altogether 14 rods in the top layer and 15 rods in the bottom layer were arranged in parallel with a distance of 4 mm between rods in each layer and a separation of both layers of 3 mm. The two layers were shifted against each other horizontally with the rods of one layer aligned with the center of the gap of adjacent rods in the opposite layer. The CYN solution was nebulized and sprayed through the electrode arrangement from the top by compressed air. In comparison to other approaches exploiting gas-phase processes, when treating water droplets, a larger overall surface area is available for the interaction with the plasma. The solution was recirculated and kept at 20 °C. Voltage and current pulses were measured with the same setup as for the corona-like discharges.

### 2.4. Plasma treatment of CYN

#### 2.4.1. CYN degradation efficacy depending on operating parameters

For the evaluation of both plasma treatment processes, the effects of operating voltage, wire diameter (corona-like discharge only) and initial solution pH on the CYN degradation efficacy were investigated. Purified CYN was diluted to a concentration of 0.45 μg $mL^{-1}$ at 250 mL of sample volume using Milli-Q water. Values for pH and electric conductivity were measured before and after the treatment. The pH was adjusted using NaOH for experiments where the effect of an elevated initial solution pH was investigated (for pH 7.5 and 9.0). The diluted CYN extract reached pH 5.0 without further pH adjustment. The sample was placed in the reservoir and circulated through the reactor before plasma application until the sample solution reached 20 °C. Plasma treatment was performed for 60 min. Aliquots of 1 mL were withdrawn from the reservoir in the recirculation system outside the reactor every 15 min and directly analyzed by HPLC-DAD for CYN concentration. The energy dissipated by individually applied high voltage pulses was determined once per experiment from recorded voltage and current waveforms by integrating their product for the duration of one pulse. The reactor was cleaned after every experiment using Milli-Q water. Experiments were repeated three times. Parameters that resulted in most effective CYN degradation were used to optimize both treatment processes for subsequent experiments unless stated otherwise.

#### 2.4.2. CYN degradation kinetics and mechanisms

Following the selection of best treatment parameters from the studied parameter range, degradation kinetics and mechanisms were investigated. Purified CYN was diluted to a concentration of 0.8 μg $mL^{-1}$ at 250 mL of sample volume in Milli-Q water. Compared to the first part of this study, a higher initial CYN concentration was used to increase the concentration of potential degradation products. To compensate the increased initial CYN concentration and to obtain a higher number of quantifiable observations, the treatment time was extended to 140 min. An aliquot of 1 mL was withdrawn every 20 min and directly quantified by HPLC-DAD for CYN concentrations. LC-MS was used to follow the formation of potential degradation products. The energy per pulse was determined every 20 min right after a sample was withdrawn.

## 3. Results and discussion

### 3.1. CYN degradation efficacy depending on operating parameters

#### 3.1.1. Corona-like plasma

In order to evaluate the CYN degradation efficacy of a pulsed corona-like discharge in water, we investigated the effects of the most pertinent operating parameters, i.e. applied voltage, initial solution pH and diameter of the high voltage electrode. Table 1 summarizes the studied parameters for both discharges and the how they affect the degradation efficacy. Electric discharges in water are known to generate reactive species including •OH, $H_2O_2$, O•, H•, electrons and photons in the UV/Vis and infrared spectrum

**Table 1**
Influence of selected treatment parameters on CYN degradation efficacy for electric discharges and conditions used in the present study.

| Discharge type | Parameter | Effect on CYN degradation efficacy |
|---|---|---|
| Corona-like discharge in water | Voltage<br>39 kV → 45 kV | + |
| | Wire diameter<br>50 μm → 80 μm | 0 |
| | Initial solution pH<br>5.0 → 7.5<br>7.5 → 9.0 | +<br>0 |
| DBD in air on top of water droplets | Voltage<br>−11 kV → −12 kV | − |
| | Initial solution pH<br>5.0 → 7.5 → 9.0 | 0 |

Note: Underlined parameters were selected for the investigation of CYN degradation kinetics and mechanisms. Symbols used: beneficial effect: +, no effect: 0, adverse effect: .

(Sun et al., 1998, 1997). Additionally, corona-like discharges in water can yield ion temperatures of about 2000 K in the discharge channels (Šunka, 2001). However, oxidation by •OH is generally considered to be the most relevant mechanism for pollutant degradation by a discharge submerged in water (Banaschik et al., 2018). The •OH readily forms $H_2O_2$ if it is not consumed in reactions with pollutants or other matrix compounds. Accordingly, $H_2O_2$ concentrations are a valuable indicator for the production of the preceding short-lived •OH (Locke and Shih, 2011).

After 1 h of plasma treatment, the production of $H_2O_2$ in the corona-like discharge system was measured in the absence of CYN and reached approximately 30 mg $H_2O_2$ $L^{-1}$. Since $H_2O_2$ could conceivably degrade CYN, a control experiment with 0.45 μg $mL^{-1}$ of CYN treated by 30 mg $L^{-1}$ of $H_2O_2$ over the course of 1 h for a pH range from 3.0 to 9.0 was conducted. Results showed that $H_2O_2$ by itself did not significantly degrade CYN ($p > 0.05$) regardless of the pH value (Supplementary Fig. S5). For a lack of information on the reactivity of O• and H• with CYN, they were not further considered for the analysis. Similarly, the free electrons from the plasma filaments were primarily considered to be associated with the formation of •OH from water (Banaschik et al., 2017; Rumbach et al., 2018). Likewise, the emitted UV radiation was assumed to result in •OH formation due to the homolytic cleavage of $H_2O_2$ (He et al., 2014b). Direct thermal CYN decomposition may have also been possible, but only in direct vicinity to the rather narrow discharge channels. Temperatures decreased fast within a distance of several hundreds of micrometers from the channels to less than 100 °C, which CYN is known to tolerate at a pH ≤ 7 (Adamski et al., 2016a). Conversely, these extreme but transient ion temperatures in the plasma filaments were more likely involved in •OH production by thermolysis of water (Song et al., 2005).

Fig. 1(A) compares the degradation of CYN by corona-like discharges operated with 35 kV and 45 kV. As shown, increasing the operating voltage from 39 kV to 45 kV resulted in increased degradation efficacy after 1 h of plasma treatment (Fig. 1(A)). According to Sun et al. (1997), this can be explained by an increasing •OH-yield for the higher operating voltage. Discharges are actually instigated and sustained by electric fields associated with electrode geometry and applied voltage. Accordingly, the diameter of the high voltage electrode may also affect reactive species generation for the same operating voltage. However, increasing the tungsten wire diameter from 50 μm to 80 μm had no significant effect on CYN degradation efficacy.

Fig. 1(B) compares CYN degradation by corona-like discharges at initial solution pH values of 5.0, 7.5 and 9.0. CYN degradation efficacy substantially increased once the initial solution pH was increased from 5.0 to 7.5 by NaOH addition. However, further increasing the pH from 7.5 to 9.0 showed no significant effect on the degradation efficacy (Fig. 1(B)). During 1 h of plasma treatment, the initial solution pH values decreased from pH 9.0 to approximately pH 8.2–8.4, from pH 7.5 to about pH 5.8 and from pH 5.0 to approximately pH 4.7. The latter was in a range for a decrease similar to what was observed for the degradation of pharmaceutical residues (Banaschik et al., 2015).

After 1 h of plasma treatment at pH 9.0, CYN concentration was below the limit of detection (2.7 ng $mL^{-1}$). The observed pH-dependency could be caused by the plasma chemistry of the corona-like discharge, i.e. the formation and reactivity of reactive

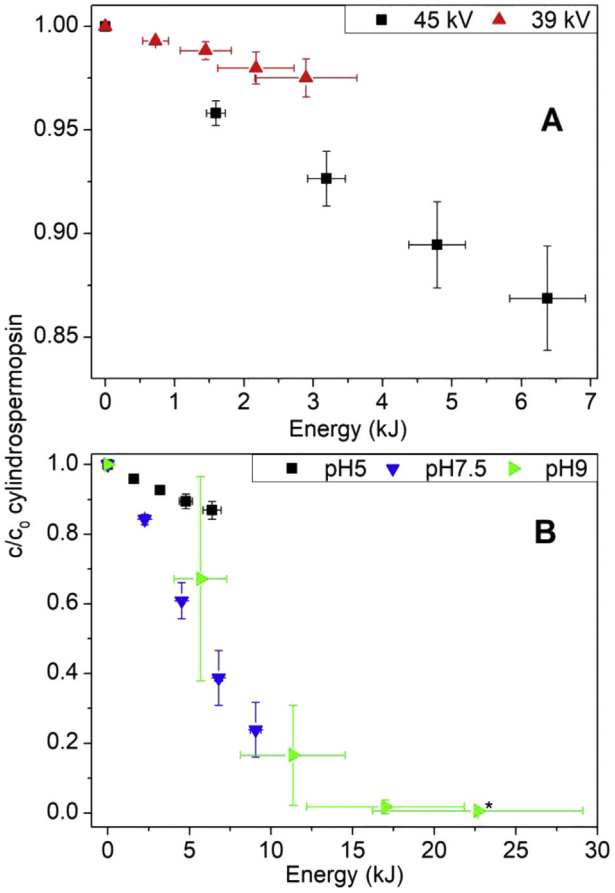


**Fig. 1.** CYN degradation efficacy for a pulsed corona-like discharge in water for two different operating voltages (graph A) and for different initial pH values for an operating voltage of 45 kV (graph B). The total treatment time was 60 min and the initial CYN concentration was 0.45 μg $mL^{-1}$ (n = 3, error bars represent standard deviations; *: < limit of detection of 2.7 ng $mL^{-1}$ CYN). Note the different scales of x- and y-axes.

species and degradation mechanisms, the speciation of CYN at elevated pH or a combination of both. The •OH yield generated by a needle-to-plate pulsed streamer corona discharge reactor submerged in water was shown to increase at neutral and slightly alkaline pH (Sun et al., 1997). In the present study, the steady-state •OH concentration ($[•OH]_{SS}$), i.e. the concentration at which •OH generation and consumption are at equilibrium, was determined using pCBA as a probe molecule. After 1 h of plasma treatment in the absence of CYN, $[•OH]_{SS}$ was not significantly different at pH 5.0 ($[•OH]_{SS} = (1.7 \pm 0.5) \times 10^{-14}$ mol $L^{-1}$) and pH 7.5 ($[•OH]_{SS} = (1.3 \pm 0.5) \times 10^{-14}$ mol $L^{-1}$). Conversely, the reactivity of •OH decreases with increasing pH as indicated by its redox potential of 2.7 V at acidic and 1.8 V at neutral pH (Buxton et al., 1988). Due to the pH-dependency of CYN degradation and •OH reactivity but similar steady-state •OH concentrations for both pH values, it is essential to consider CYN speciation and other oxidative chemical species and mechanisms. The $pK_a$ of CYN was estimated to be 8.8 (Onstad et al., 2007), resulting in deprotonation at more alkaline pH. However, because •OH usually reacts very fast with organic compounds, Onstad et al. (2007) assumed the effect of solution pH on the reaction of •OH with CYN to be insignificant.

The observed pseudo zeroth order rate constants for the degradation of CYN by pulsed corona-like discharges were plotted against the solution pH in Fig. 2. Additionally, the speciation of CYN with respect to the solution pH is shown. For the pH-dependent ozonation of CYN, Onstad et al. (2007) reported an exponential increase of the observed rate constant with increasing solution pH. Consequently, a similar characteristic can be expected if the pH-dependency is caused by the toxin speciation. Instead, when using a pulsed corona-like discharge for CYN degradation, observed rate constants rather followed a sigmoidal trend (Fig. 2). Altogether, this still confirmed a pH-dependent CYN degradation when the solution pH was elevated from 5.0 to 7.5, but an independency from the solution pH for a further increase to pH 9.0. In combination with the aforementioned decline in reactivity of •OH at neutral and alkaline pH and deprotonation of CYN at alkaline pH, Fig. 2 may indicate the formation of other, long-lived reactive species or degradative mechanisms at neutral and alkaline pH. As shown by Adamski et al. (2016b), direct CYN photodegradation by the produced UV radiation could explain the higher CYN removal when the solution pH was increased from 5.0 to 7.5. However, CYN degradation should have further increased as the solution pH became more alkaline, i.e. pH 9.0 (Adamski et al., 2016b), which was not observed in our study. In an attempt to further investigate pH-dependency, CYN solutions were adjusted to pH 3.0 and 12.0

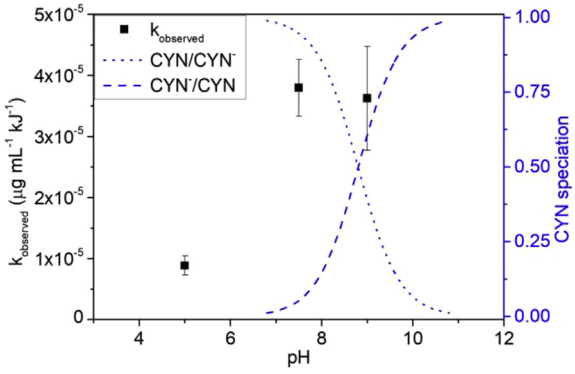


**Fig. 2.** Dependency of pH for observed rate constants for CYN degradation by a pulsed corona-like discharge in water assuming a pseudo zeroth order reaction. Dotted and dashed lines show the ratio of protonated to deprotonated CYN and vice versa (calculated from $pK_a = 8.8$).

which resulted in an increase of electric conductivity by a factor of >10 and >100, respectively, which substantially and adversely affected the possibility to sustain discharges at a peak voltage that was comparable to the previous experiments. Nevertheless, this allowed us to infer that toxin speciation at neutral and alkaline pH did not cause the observed pH-dependent effect.

After 15 min of plasma treatment at pH ≥ 7.5, CYN degradation still continued without further plasma application, further supporting the assumption of the formation of other, long-lived oxidative species and degradative mechanisms. This residual oxidative effect appeared to be pH-dependent, as the effect was more pronounced at pH 9.0 and acidification of a sample taken after 15 min of plasma treatment inhibited further CYN degradation. Residual disinfective effects of plasma treated water were observed in other studies for different discharge systems, in which $O_3$, $H_2O_2$ and peroxynitrous acid ($HNO_3$) were identified as long-lived microbicidal agents (Scholtz et al., 2015). A residual oxidative effect of plasma treated water was recently shown to last for at least four days (Nisol et al., 2019), but strongly depends on different parameters such as water conductivity, temperature, pH and composition, as well as type and quantity of reactive species. However, $O_3$ and $HNO_3$ were not produced in appreciable amounts by an electric discharge submerged in water that was similar to our experimental setup (Banaschik et al., 2015). Moreover, admixture of $H_2O_2$ by itself was not observed to yield appreciable degradation of CYN. When using a stainless steel instead of a titanium mesh for the ground electrode, Banaschik et al. (2017) observed a 75% higher degradation of phenol in a corona-like discharge in water due to the contribution of Fenton's reaction. The corrosion of the ground electrode led to the dissolution of iron which could subsequently react with $H_2O_2$ in a Fenton reaction and improved pollutant degradation (Banaschik et al., 2017). Similarly, the high voltage electrode is also expected to corrode and consequently, tungsten may dissolve, get oxidized to tungstate and catalyze $H_2O_2$ oxidation of CYN (Floor et al., 1989). However, optimal pH for both reactions is usually reported to be in the acidic range (Floor et al., 1989; Park et al., 2017) whereas the degradation of CYN observed in this study increased at alkaline pH and was inhibited at acidic pH. Lee et al. (2013) observed substantial oxidation of the dye Reactive Black 5 and As(V) in a Fenton reaction under alkaline conditions, hypothesizing the formation of oxidants other than •OH, namely high-valent iron complexes. We thus hypothesize that other reactive species, which are more stable and reactive at neutral and alkaline pH, are formed in the corona-like discharge in water under these conditions. Examples for other reactive species or mechanisms are the aforementioned tungstate-catalyzed $H_2O_2$ oxidation, Fenton reaction and high-valent iron complexes as well as other reactive oxygen species such as superoxide anion radicals which are formed as a product of •OH and $H_2O_2$ reaction (Banaschik et al., 2017). As for the pH-dependency, the produced UV radiation would not have caused a residual oxidation in form of direct CYN photodegradation, as this process is instantaneous and was not sustained without plasma application. Further experiments are required to clearly characterize the cause of pH-dependent CYN degradation and the residual oxidative effect of plasma treated water.

### 3.1.2. DBD plasma

In order to evaluate CYN degradation efficacy of a pulsed DBD in air around water droplets, the effects of operating voltage and initial solution pH were investigated (Table 1). A DBD in air at atmospheric pressure produces primarily $O_3$, and, in addition, oxygen ions such as $O_2^-$ and $O_3^-$, $NO_x$ as well as electrons and photons (Kogelschatz et al., 1988; Pekárek, 2012). Since the sample solution was directly nebulized into the discharge chamber, minor

quantities of •OH and $H_2O_2$ were also produced by the electric discharges at the air-water interface of the water droplets and by the decomposition of dissolved $O_3$. The formation of $H_2O_2$ in the DBD after 1 h of plasma treatment and in the absence of CYN was determined with approximately 2.9 mg $L^{-1}$. Again, $H_2O_2$ served as an indicator for the generation of •OH (Locke and Shih, 2011). However, the amount of $H_2O_2$, produced by the DBD, was comparatively low and approximately one tenth of the amount produced by the corona-like discharge. Therefore, CYN oxidation by •OH was assumed to be negligible for the DBD treatment. Correspondingly, more direct plasma mechanisms, such as electron impact on water molecules, which is essential for the corona-like discharge, contributed to a much lesser degree to the generation of radical species, in particular •OH.

Fig. 3 compares CYN degradation by a DBD in air around water droplets operated at −12 kV and −11 kV. This is a small but important difference for the operation of this DBD. In contrast to the corona-like discharge, CYN degradation efficacy in the DBD decreased when operating voltage was increased (Fig. 3). For a DBD in air at atmospheric pressure, oxygen consumption in $NO_x$ reactions becomes more effective than $O_3$ production when exceeding a certain voltage threshold. Moreover, $O_3$ can be depleted by reactions involving N and NO (Kogelschatz et al., 1988). Even though the quantity of $NO_x$ and related compounds increased with higher operating voltage, CYN degradation efficacy decreased, confirming assumptions that CYN oxidation in the DBD was dominated by $O_3$.

In contrast to what Onstad et al. (2007) observed, CYN ozonation using a DBD appeared to be pH-independent when increasing the initial solution pH from 5.0 to 7.5 and to 9.0 (Table 1). Similar to the corona-like discharge, direct photodegradation by the produced UV light could have contributed to CYN degradation at neutral and alkaline solution pH. However, due to the formation of $NO_x$, the solution pH substantially decreased throughout the treatment. When starting with an initial pH of 9.0, the solution pH dropped to approximately 3.5 after 1 h of plasma treatment. A pH-buffer was not used, because the electric conductivity of the solution would have increased and consequently made it impossible to ignite discharges at the same peak voltage and pulse duration as for lower conductivities. Accordingly, the effect of solution pH on the CYN degradation efficacy in a DBD could not be unambiguously characterized. Other approaches, e.g. operating the DBD with oxygen instead of air to avoid $NO_x$ formation and associated solution acidification, would have changed the entire system and results would not be comparable. Nevertheless, the rapid acidification of the solution further supports the hypothesis that •OH only plays a minor role in the degradation of CYN, since aqueous $O_3$ is more stable at acidic pH, lowering the formation of •OH as a result of $O_3$ decomposition in water.

### 3.2. CYN degradation kinetics and mechanisms

After the optimal treatment parameters for both approaches had been identified with respect to the studied parameter range, CYN degradation kinetics and mechanisms were investigated in more detail. Treatment parameters corresponding to the highest efficacy were chosen for the optimization of both discharges (Table 1), except for the initial ideal solution pH that was found for the corona-like discharge. Data obtained for CYN degradation at pH 9.0 showed more variability as indicated by the standard deviations in Fig. 1(B). Since the assessment of degradation kinetics requires a higher number of quantifiable observations, but CYN concentrations were already reduced close to the analytical detection limit during 60 min of treatment at pH 9.0, pH 7.5 was chosen for additional experiments. CYN degradation efficacy $E_{CYN}$ was calculated using equation (1) (adapted from Banaschik et al., 2017).

$$E_{CYN} = k \times c_0^i \times 3,600 \quad (1)$$

where k is the observed rate constant in $\mu g^{1-i}\ mL^{i-1}\ kJ^{-1}$, $c_0$ is the initial CYN concentration in $\mu g\ mL^{-1}$, i is the order of reaction and 3600 is a factor for unit conversion from $kJ^{-1}$ to $kWh^{-1}$.

Fig. 4 compares CYN degradation by a corona-like discharge submerged in water and a DBD in air around water droplets under optimized conditions and Table 2 summarizes the determined kinetic data and CYN degradation efficacy of both treatment processes. CYN degradation was more effective for the corona-like discharge in water following pseudo first order reaction with $0.24 \pm 0.02$ g $kWh^{-1}\ L^{-1}$ in comparison to the DBD in air with water droplets following a pseudo zeroth order reaction with $0.03 \pm 0.00$ g $kWh^{-1}\ L^{-1}$ (Fig. 4 and Table 2). CYN degradation efficacies will certainly improve following further technical optimizations of the plasma treatment processes. However, the scope of this study was to provide a basic understanding of prospective but conceptually different plasma methods to guide efforts for future developments. In both discharge systems, oxidative species are

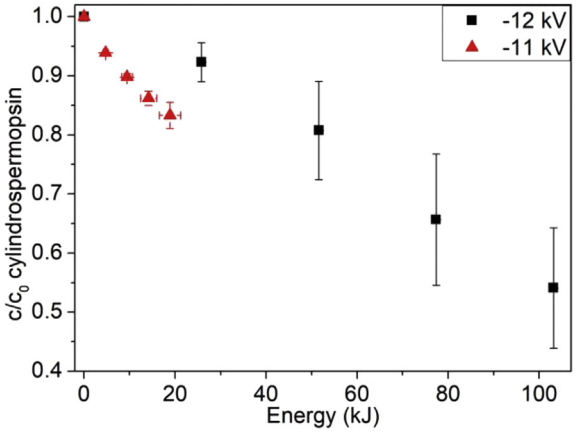


**Fig. 3.** CYN degradation efficacy for a pulsed DBD in air with water droplets for two different operating voltages. The total treatment time was 60 min and the initial CYN concentration was 0.45 μg $mL^{-1}$ (−12 kV: n = 3, −11 kV: n = 2, error bars represent standard deviations).

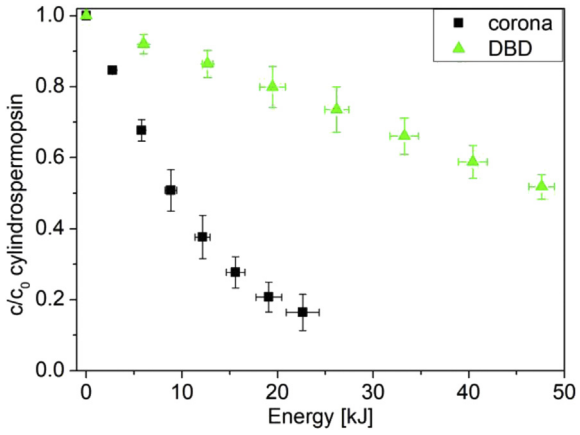


**Fig. 4.** Comparison of CYN degradation efficacy in a pulsed corona-like discharge in water and a pulsed DBD in air with water droplets for best treatment parameters found in this study for a total treatment time of 140 min and an initial CYN concentration of 0.8 μg $mL^{-1}$ (n = 3, error bars represent standard deviations).

**Table 2**
Data on reaction kinetics and calculated CYN degradation efficacy for the best treatment parameters in the investigated parameter range (n = 3, mean ± standard deviation).

| Discharge type | Reaction order | Observed rate constant k | Half-life $E_{1/2}$ [kJ] | Degradation efficacy $E_{CYN}$ [g $kWh^{-1}$ $L^{-1}$] |
|---|---|---|---|---|
| Corona-like discharge in water | Pseudo 1st order | $(8.4 \pm 0.8) \times 10^{-2} kJ^{-1}$ | 8.3 ± 0.7 | 0.24 ± 0.02 |
| DBD in air with water droplets | Pseudo $0^{th}$ order | $(7.9 \pm 0.9) \times 10^{-3}$ μg $mL^{-1}$ $kJ^{-1}$ | 50.4 ± 5.4 | 0.03 ± 0.00 |

continuously produced as long as voltage is supplied. Thus, differences in the degradation efficacies may have been caused by quantity and reactivity of the produced oxidative species, but also by the frequency of encounters with toxin molecules. Correspondingly, Onstad et al. (2007) reported apparent rate constants for oxidation by •OH being higher by a factor of $10^4$ compared to oxidation by $O_3$. Hence, •OH were shown to have a higher reactivity with CYN compared with $O_3$. CYN degradation in the corona-like discharge was mainly caused by •OH and, especially at neutral and alkaline pH, by other, as yet unidentified reactive species. Conversely, toxin oxidation by the DBD was primarily driven by $O_3$, whereas •OH only played a minor role, which may have caused the different degradation efficacies. However, besides the reactivity of the oxidative species with the toxin, the observed reaction kinetics provide additional insight into the degradation process. The observed pseudo first order reaction for the corona-like treatment implied that the degradation rate depended on the concentration of one of the reaction partners. Since the reactive species were continuously produced as long as high voltage was supplied to the system, CYN had to be the dependent variable. The pseudo zeroth order reaction for the DBD treatment indicated that the degradation is independent from the concentration of both, CYN and the produced reactive species. In this case, the reaction was diffusion-controlled, i.e. the rate determining step was the frequency of encounters of reactive species with toxin molecules. The majority of reactive species was produced in the gaseous phase, while the toxin remained dissolved in the liquid phase. CYN degradation was thus restricted to reactions at the air-water interface and in the solution, which in turn was limited by the solubility of $O_3$ in water and consequently lower concentrations. In comparison, for the corona-like discharge, reactive species were directly produced in the aqueous phase – the same phase CYN was dissolved in. Furthermore, thorough mixing was ensured by the continuous flow of the solution through the plasma reactor, consequently increasing the frequency of encounters between reactive species and toxin molecules. Therefore, our results implied that the degradation efficacy was determined by plasma-chemical processes of both discharges, especially type and reactivity of produced oxidative species as well as if they were produced in the same phase as CYN.

In order to assess the different degradation mechanisms for the predominant generation of •OH and $O_3$ by the corona-like discharge and DBD, respectively, HPLC-MS was employed to follow the formation of potential CYN degradation products. Following criteria were used to qualify a chromatographic peak as potential product (Antoniou et al., 2008): peaks had to have a signal to noise ratio of ≥3 and, if the same peak appeared in the untreated sample as well, the peak area had to be at least two times higher in the treated sample. Using this rule, multiple product peaks were identified after 140 min treatment for both methods (Supplementary Figs. S6 and S7). However, the purity of CYN used for the experiments was estimated to be approximately 70%. Therefore, detected *m/z* could not be unambiguously associated solely with CYN degradation products. Table 3 compares products detected in our study with information reported in the literature. Only four products were also observed in other studies (Table 3). For the products *m/z* = 432.0 and *m/z* = 308.0, the reactive species responsible for the degradation appeared to be different. However, dissolved $O_3$ could decompose to •OH and the functional moieties under attack could therefore qualitatively although not quantitatively then have been the same for both species, resulting in identical degradation products.

When comparing the chromatograms of CYN after 140 min of treatment by a corona-like discharge and a DBD, four and five peaks, respectively, were found to be substantially different (Supplementary Fig. S8). One of the product peaks (*m/z* = 485.0) appeared in the chromatograms of both treatment methods, but the peak area was at least one order of magnitude larger for the DBD treatment compared to the corona-like discharge treatment. Another peak appeared at the same retention time (0.5 min), but represented two different products with *m/z* = 240.0 and *m/z* = 306.0 for the corona-like discharge and DBD, respectively. One distinctive product peak (*m/z* = 330.0) could only be seen in the chromatogram for the corona-like discharge, whereas two other distinctive product peaks (*m/z* = 439.0 and *m/z* = 481.0) appeared only for the DBD treatment. Chemical structures for the products with *m/z* of 432.0, 308.0, 306.0 and 240.0 have been proposed in the literature cited in Table 3. For products newly detected in the present work, more analytical work would help to elucidate their chemical structures. Even though the *m/z* of the product peaks could not definitively be associated solely with CYN degradation products, these differences indicate distinct CYN degradation mechanisms in both discharges based on the formation of different reactive species.

Especially in the context of drinking water treatment, the toxicity of the treated CYN solution, i.e. production of potentially toxic degradation products, is an important aspect that needs to be considered. Banker et al. (2001) detected two major degradation products following chlorine treatment of CYN, namely 5-chloro-CYN and cylindrospermopsic acid, in which the uracil moiety was altered or removed. Both degradation products were non-toxic with $LD_{50}$ > 10,000 μg $kg^{-1}$ after five days of intraperitoneal injection in mice, while the $LD_{50}$ of CYN was 200 μg $kg^{-1}$. The uracil moiety thus seemed to be essential for the toxicity of CYN (Banker et al., 2001), and, indeed, many CYN degradation studies reported the uracil moiety to be susceptible to oxidation. In fact, Song et al. (2012) determined that 84% of •OH, produced by the radiolysis of water, initially reacted with CYN's uracil moiety. Similarly, the uracil moiety in CYN was also reported to be the most susceptible site for reactions with $O_3$ (Onstad et al., 2007; Yan et al., 2016). All four degradation products detected in the present study that were also reported by others (Table 3) corresponded to tentatively identified compounds in which the uracil moiety was altered (*m/z = 432.0*; hydroxylation of CYN, likely to occur at the uracil moiety) or completely removed (*m/z = 308.0, 306.0, 240.0*; following a series of reactions) (He et al., 2014b; Yan et al., 2016). Therefore, it can be hypothesized that CYN treatment by corona-like discharge and DBD processes most likely yielded non- or at least less toxic degradation products in comparison to the untreated CYN.

## 4. Conclusions

CYN was effectively degraded using two different NTPs. CYN degradation was found to be more effective for a corona-like discharge submerged in water compared to a DBD operated in air

**Table 3**
Comparison of CYN degradation products (*m/z*) detected in the present study with the literature. Predominantly produced reactive species are underlined.

| *m/z* detected as $[M+H]^+$ | Discharge type | Treatment method used in the cited studies |
|---|---|---|
| 432.0 | DBD → $\underline{O_3}$ | $UV/H_2O_2$ → $\underline{\bullet OH}$ (He et al., 2014b) |
| 308.0 | Corona-like → $\underline{\bullet OH}$ | Ozonation → $\underline{O_3}$ (Yan et al., 2016) |
| 306.0 | DBD → $\underline{O_3}$ | Ozonation → $\underline{O_3}$ (Yan et al., 2016) |
| 240.0 | Corona-like → $\underline{\bullet OH}$ | $UV/H_2O_2$ → $\underline{\bullet OH}$ (He et al., 2014b) |

with water droplets. Both methods, rely on the generation of different reactive species and might hence offer different advantages with respect to application in water treatment. Especially the corona-like discharge submerged in water can be very attractive in case of high natural organic matter concentrations and the presence of chlorine or bromide. Because the main reactive species produced by the discharge was •OH, the risk of toxic disinfection byproduct production could be substantially reduced. Parameters that were not studied here (such as electrode material, sample matrix composition, gas type and flow, and reactor design) may also affect degradation efficacy, i.e. reaction times and energy demands. The notable residual oxidation in water after corona-like discharge plasma treatment due to longer-lived reactive species or other degradative mechanisms may have interesting implications for drinking water treatment. This depot can guarantee an ongoing disinfection in the distribution system, just like chlorine but without the unpleasant taste and odor, and therefore be attractive for drinking water suppliers. However, associated potential disadvantages or risks, such as water acidification or potential toxicity to consumers, need to be carefully considered and studied in more detail. Nevertheless, the presented study provides a basic understanding of the interaction of NTPs with CYN, confirms the potential of innovative NTP technologies for drinking water treatment, and encourages future efforts on scaling up and investigations in relevant environments.

## CRediT authorship contribution statement

**Marcel Schneider:** Conceptualization, Methodology, Validation, Formal analysis, Investigation, Resources, Writing - original draft, Visualization, Project administration. **Raphael Rataj:** Methodology, Validation, Formal analysis, Investigation, Writing - review & editing, Visualization. **Juergen F. Kolb:** Conceptualization, Methodology, Resources, Writing - review & editing, Supervision, Funding acquisition. **Ludek Bláha:** Conceptualization, Resources, Writing - review & editing, Supervision, Funding acquisition.

## Declaration of competing interest

The authors declare that they have no known competing financial interests or personal relationships that could have appeared to influence the work reported in this paper.

## Acknowledgement

This research received funding from the European Union's Horizon 2020 research and innovation program under the Marie Skłodowska-Curie grant agreement No. 722493 NaToxAq, from the RECETOX Research Infrastructure grant LM2018121 from the Czech Ministry of Education, Youth and Sports, and CETOCOEN EXCELLENCE Teaming 2 project supported by European Union's Horizon 2020 (857560) and Czech Ministry of Education, Youth and Sports (CZ02.1.01/0.0/0.0/18_046/0015975). Any opinions expressed in this article only reflect the authors' views and the European Union's Research Executive Agency is not responsible for any use that may be made of the information it contains. We would like to thank Dr. Lucie Bláhová, Hana Klimová and Dr. Katja Zocher for their assistance and advice in the laboratory and David Konečný for constructive criticism on the manuscript.

## Appendix A. Supplementary data

Supplementary data to this article can be found online at https://doi.org/10.1016/j.envpol.2020.115423.

## References

Adamski, M., Żmudzki, P., Chrapusta, E., Bober, B., Kaminski, A., Zabaglo, K., Latkowska, E., Bialczyk, J., 2016a. Effect of pH and temperature on the stability of cylindrospermopsin. Characterization of decomposition products. Algal Res. 15, 129–134. https://doi.org/10.1016/J.ALGAL.2016.02.020.

Adamski, M., Żmudzki, P., Chrapusta, E., Kaminski, A., Bober, B., Zabaglo, K., Bialczyk, J., 2016b. Characterization of cylindrospermopsin decomposition products formed under irradiation conditions. Algal Res. 18, 1–6. https://doi.org/10.1016/J.ALGAL.2016.05.027.

Antoniou, M.G., Shoemaker, J.A., de la Cruz, A.A., Dionysiou, D.D., 2008. LC/MS/MS structure elucidation of reaction intermediates formed during the TiO2 photocatalysis of microcystin-LR. Toxicon 51, 1103–1118. https://doi.org/10.1016/J.TOXICON.2008.01.018.

Bakheet, B., Islam, M.A., Beardall, J., Zhang, X., McCarthy, D., 2018. Electrochemical inactivation of Cylindrospermopsis raciborskii and removal of the cyanotoxin cylindrospermopsin. J. Hazard Mater. 344, 241–248. https://doi.org/10.1016/J.JHAZMAT.2017.10.024.

Banaschik, R., Jablonowski, H., Bednarski, P.J., Kolb, J.F., 2018. Degradation and intermediates of diclofenac as instructive example for decomposition of recalcitrant pharmaceuticals by hydroxyl radicals generated with pulsed corona plasma in water. J. Hazard Mater. 342, 651–660. https://doi.org/10.1016/J.JHAZMAT.2017.08.058.

Banaschik, R., Lukes, P., Jablonowski, H., Hammer, M.U., Weltmann, K.-D., Kolb, J.F., 2015. Potential of pulsed corona discharges generated in water for the degradation of persistent pharmaceutical residues. Water Res. 84, 127–135. https://doi.org/10.1016/J.WATRES.2015.07.018.

Banaschik, Robert, Lukes, P., Miron, C., Banaschik, Richard, Pipa, A.V., Fricke, K., Bednarski, P.J., Kolb, J.F., 2017. Fenton chemistry promoted by sub-microsecond pulsed corona plasmas for organic micropollutant degradation in water. Electrochim. Acta 245, 539–548. https://doi.org/10.1016/J.ELECTACTA.2017.05.121.

Banker, R., Carmeli, S., Werman, M., Teltsch, B., Porat, R., Sukenik, A., 2001. Uracil moiety is required for toxicity of the cyanobacterial hepatotoxin cylindrospermopsin. J. Toxicol. Environ. Health. A 62, 281–288. https://doi.org/10.1080/009841001459432.

Blahova, L., Oravec, M., Marsalek, B., Sejnohova, L., Simek, Z., Blaha, L., 2009. The first occurrence of the cyanobacterial alkaloid toxin cylindrospermopsin in the Czech Republic as determined by immunochemical and LC/MS methods. Toxicon 53, 519–524. https://doi.org/10.1016/j.toxicon.2009.01.014.

Brooks, B.W., Lazorchak, J.M., Howard, M.D.A., Johnson, M.-V.V., Morton, S.L., Perkins, D.A.K., Reavie, E.D., Scott, G.I., Smith, S.A., Steevens, J.A., 2016. Are harmful algal blooms becoming the greatest inland water quality threat to public health and aquatic ecosystems? Environ. Toxicol. Chem. 35, 6–13. https://doi.org/10.1002/etc.3220.

Buxton, G.V., Greenstock, C.L., Helman, W.P., Ross, A.B., 1988. Critical Review of rate constants for reactions of hydrated electrons, hydrogen atoms and hydroxyl radicals (•OH/•O−) in Aqueous Solution. J. Phys. Chem. Ref. Data 17, 513–886. https://doi.org/10.1063/1.555805.

Cerasino, L., Meriluoto, J., Bláha, L., Carmeli, S., Kaloudis, T., Mazur-Marzec, H., 2016. Extraction of cyanotoxins from cyanobacterial biomass. In: Meriluoto, J., Spoof, L., Codd, G.A. (Eds.), Handbook of Cyanobacterial Monitoring and Cyanotoxin Analysis. John Wiley & Sons, Ltd., pp. 350–353 https://doi.org/https://doi.org/10.1002/9781119068761.ch38.

Dixon, M.B., Falconet, C., Ho, L., Chow, C.W.K., O'Neill, B.K., Newcombe, G., 2011. Removal of cyanobacterial metabolites by nanofiltration from two treated waters. J. Hazard Mater. 188, 288–295. https://doi.org/10.1016/J.JHAZMAT.2011.01.111.

Floor, M., Schenk, K.M., Kieboom, A.P.G., van Bekkum, H., 1989. Oxidation of

maltodextrins and starch by the system tungstate-hydrogen peroxide. Starch - Stärke 41, 303–309. https://doi.org/10.1002/star.19890410806.
Griffiths, D.J., Saker, M.L., 2003. The Palm Island mystery disease 20 years on: a review of research on the cyanotoxin cylindrospermopsin. Environ. Toxicol. 18, 78–93. https://doi.org/10.1002/tox.10103.
He, X., de la Cruz, A.A., O'Shea, K.E., Dionysiou, D.D., 2014a. Kinetics and mechanisms of cylindrospermopsin destruction by sulfate radical-based advanced oxidation processes. Water Res. 63, 168–178. https://doi.org/10.1016/J.WATRES.2014.06.004.
He, X., Zhang, G., de la Cruz, A.A., O'Shea, K.E., Dionysiou, D.D., 2014b. Degradation mechanism of cyanobacterial toxin cylindrospermopsin by hydroxyl radicals in homogeneous UV/H2O2 process. Environ. Sci. Technol. 48, 4495–4504. https://doi.org/10.1021/es403732s.
Ho, L., Slyman, N., Kaeding, U., Newcombe, G., 2008. Optimizing PAC and chlorination practices for cylindrospermopsin removal. J. Am. Water Works Assoc. 100, 88–96. https://doi.org/10.1002/j.1551-8833.2008.tb09776.x.
Ho, L., Tang, T., Hoefel, D., Vigneswaran, B., 2012. Determination of rate constants and half-lives for the simultaneous biodegradation of several cyanobacterial metabolites in Australian source waters. Water Res. 46, 5735–5746. https://doi.org/10.1016/J.WATRES.2012.08.003.
Ibelings, B.W., Bormans, M., Fastner, J., Visser, P.M., 2016. CYANOCOST special issue on cyanobacterial blooms: synopsis—a critical review of the management options for their prevention, control and mitigation. Aquat. Ecol. 50, 595–605. https://doi.org/10.1007/s10452-016-9596-x.
Jo, J.-O., Jwa, E., Mok, Y.-S., 2016. Decomposition of aqueous anatoxin-a using underwater dielectric barrier discharge plasma created in a porous ceramic tube. J. Korean Soc. Water Wastewater 30, 167–177. https://doi.org/10.11001/jksww.2016.30.2.167.
Klitzke, S., Beusch, C., Fastner, J., 2011. Sorption of the cyanobacterial toxins cylindrospermopsin and anatoxin-a to sediments. Water Res. 45, 1338–1346. https://doi.org/10.1016/J.WATRES.2010.10.019.
Kogelschatz, U., Eliasson, B., Hirth, M., 1988. Ozone generation from oxygen and air: discharge physics and reaction mechanisms. Ozone Sci. Eng. 10, 367–377. https://doi.org/10.1080/01919518808552391.
Lee, H., Lee, H.-J., Sedlak, D.L., Lee, C., 2013. pH-Dependent reactivity of oxidants formed by iron and copper-catalyzed decomposition of hydrogen peroxide. Chemosphere 92, 652–658. https://doi.org/10.1016/J.CHEMOSPHERE.2013.01.073.
Liu, J., Hernández, S.E., Swift, S., Singhal, N., 2018. Estrogenic activity of cylindrospermopsin and anatoxin-a and their oxidative products by FeIII-B*/H2O2. Water Res. 132, 309–319. https://doi.org/10.1016/J.WATRES.2018.01.018.
Locke, B.R., Shih, K.-Y., 2011. Review of the methods to form hydrogen peroxide in electrical discharge plasma with liquid water. Plasma Sources Sci. Technol. 20, 034006 https://doi.org/10.1088/0963-0252/20/3/034006.
Magureanu, M., Bradu, C., Parvulescu, V.I., 2018. Plasma processes for the treatment of water contaminated with harmful organic compounds. J. Phys. D Appl. Phys. 51, 313002. https://doi.org/10.1088/1361-6463/aacd9c.
Ministry of Health, 2017. Guidelines for Drinking-Water Quality Management for New Zealand, third ed. Ministry of Health, Wellington.
Nisol, B., Watson, S., Leblanc, Y., Moradinejad, S., Wertheimer, M.R., Zamyadi, A., 2019. Cold plasma oxidation of harmful algae and associated metabolite BMAA toxin in aqueous suspension. Plasma Process. Polym. 16, 1800137. https://doi.org/10.1002/ppap.201800137.
Onstad, G.D., Strauch, S., Meriluoto, J., Codd, G.A., Von Gunten, U., 2007. Selective oxidation of key functional groups in cyanotoxins during drinking water ozonation. Environ. Sci. Technol. 41, 4397–4404. https://doi.org/10.1021/es0625327.
Park, J.-A., Yang, B., Park, C., Choi, J.-W., van Genuchten, C.M., Lee, S.-H., 2017. Oxidation of microcystin-LR by the Fenton process: kinetics, degradation intermediates, water quality and toxicity assessment. Chem. Eng. J. 309, 339–348. https://doi.org/10.1016/j.cej.2016.10.083.
Pekárek, S., 2012. Experimental study of surface dielectric barrier discharge in air and its ozone production. J. Phys. D Appl. Phys. 45, 75201. https://doi.org/10.1088/0022-3727/45/7/075201.
Rodríguez, E., Onstad, G.D., Kull, T.P.J., Metcalf, J.S., Acero, J.L., von Gunten, U., 2007. Oxidative elimination of cyanotoxins: comparison of ozone, chlorine, chlorine dioxide and permanganate. Water Res. 41, 3381–3393. https://doi.org/10.1016/J.WATRES.2007.03.033.
Rumbach, P., Bartels, D.M., Go, D.B., 2018. The penetration and concentration of solvated electrons and hydroxyl radicals at a plasma-liquid interface. Plasma Sources Sci. Technol. 27, 115013. https://doi.org/10.1088/1361-6595/aaed07.
Schiavon, M., Torretta, V., Casazza, A., Ragazzi, M., 2017. Non-thermal plasma as an innovative option for the abatement of volatile organic compounds: a review. Water, Air, Soil Pollut. 228, 388. https://doi.org/10.1007/s11270-017-3574-3.
Scholtz, V., Pazlarova, J., Souskova, H., Khun, J., Julak, J., 2015. Nonthermal plasma — a tool for decontamination and disinfection. Biotechnol. Adv. 33, 1108–1119. https://doi.org/10.1016/J.BIOTECHADV.2015.01.002.
Song, W., Teshiba, T., Rein, K., O'Shea, K.E., 2005. Ultrasonically induced degradation and detoxification of microcystin-LR (cyanobacterial toxin). Environ. Sci. Technol. 39, 6300–6305. https://doi.org/10.1021/es048350z.
Song, W., Yan, S., Cooper, W.J., Dionysiou, D.D., O'Shea, K.E., 2012. Hydroxyl radical oxidation of cylindrospermopsin (cyanobacterial toxin) and its role in the photochemical transformation. Environ. Sci. Technol. 46, 12608–12615. https://doi.org/10.1021/es302458h.
Sun, B., Sato, M., Clements, J.S., 1997. Optical study of active species produced by a pulsed streamer corona discharge in water. J. Electrost. 39, 189–202. https://doi.org/10.1016/S0304-3886(97)00002-8.
Sun, B., Sato, M., Harano, A., Clements, J.S., 1998. Non-uniform pulse discharge-induced radical production in distilled water. J. Electrost. 43, 115–126. https://doi.org/10.1016/S0304-3886(97)00166-6.
Šunka, P., 2001. Pulse electrical discharges in water and their applications. Phys. Plasmas 8, 2587–2594. https://doi.org/10.1063/1.1356742.
Vanova, T., Raska, J., Babica, P., Sovadinova, I., Kunova Bosakova, M., Dvorak, P., Blaha, L., Rotrekl, V., 2019. Freshwater cyanotoxin cylindrospermopsin has detrimental stage-specific effects on hepatic differentiation from human embryonic stem cells. Toxicol. Sci. 168, 241–251. https://doi.org/10.1093/toxsci/kfy293.
Westrick, J.A., Szlag, D., 2018. A cyanotoxin primer for drinking water professionals. J. AWWA (Am. Water Works Assoc.) 110, E1–E16. https://doi.org/10.1002/awwa.1088.
WHO, 2020. Drinking-water Quality Guidelines [WWW Document]. https://www.who.int/water_sanitation_health/water-quality/guidelines/en/. (Accessed 27 March 2020).
Wu, C.-C., Huang, W.-J., Ji, B.-H., 2015. Degradation of cyanotoxin cylindrospermopsin by TiO2-assisted ozonation in water. J. Environ. Sci. Health. A. Toxiol. Hazard. Subst. Environ. Eng. 50, 1116–1126. https://doi.org/10.1080/10934529.2015.1047664.
Xia, T., Kleinheksel, A., Lee, E.M., Qiao, Z., Wigginton, K.R., Clack, H.L., 2019. Inactivation of airborne viruses using a packed bed non-thermal plasma reactor. J. Phys. D Appl. Phys. 52, 255201. https://doi.org/10.1088/1361-6463/ab1466.
Yan, S., Jia, A., Merel, S., Snyder, S.A., O'Shea, K.E., Dionysiou, D.D., Song, W., 2016. Ozonation of cylindrospermopsin (cyanotoxin): degradation mechanisms and cytotoxicity assessments. Environ. Sci. Technol. 50, 1437–1446. https://doi.org/10.1021/acs.est.5b04540.
Zhang, G., He, X., Nadagouda, M.N., O'Shea K, E., Dionysiou, D.D., 2015. The effect of basic pH and carbonate ion on the mechanism of photocatalytic destruction of cylindrospermopsin. Water Res. 73, 353–361. https://doi.org/10.1016/J.WATRES.2015.01.011.
Zhang, Y., Wei, H., Xin, Q., Wang, M., Wang, Qi, Wang, Qiang, Cong, Y., 2016. Process optimization for microcystin-LR degradation by Response Surface Methodology and mechanism analysis in gas–liquid hybrid discharge system. J. Environ. Manag. 183, 726–732. https://doi.org/10.1016/j.jenvman.2016.09.030.